*FRENCH-UKRAINIAN JOURNAL OF CHEMISTRY (**2015**, VOLUME **3**, ISSUE **1**)*

Effect of ligand substitution in $[Fe(H\text{-}trz)_2(trz)]BF_4$ spin crossover nanoparticles

Iurii Suleimanov[a,b], José Sanchez Costa[b], Gábor Molnár[b], Lionel Salmon[b*], Igor O. Fritsky[a] and Azzedine Bousseksou[b]

[a] *Department of Chemistry, Taras Shevchenko National University of Kyiv, Volodymyrska Street, 64/13, Kyiv 01601, Ukraine*

[b] *Laboratoire de Chimie de Coordination, CNRS & Université de Toulouse (INPT, UPS), 205 Route de Narbonne, 31400, Toulouse, France*

contacting e-mail lionel.salmon@lcc-toulouse.fr

Keywords: *spin crossover, reverse microemulsions, nanoparticles, ligand substitution.*

Spin crossover iron(II) 1,2,4-triazole-based coordination compounds in the form of nanoparticles were prepared using a reverse microemulsion technique. Ligand substitution approach was applied to decrease the spin crossover temperature towards room temperature in the well-known $[Fe(H\text{-}trz)_2(trz)]BF_4$ complex. The compositions of the particles were determined by elemental analysis and thermogravimetry. The morphology was monitored by transition electron microscopy (TEM). The effect associated with the ligand substitution was investigated by optical and magnetic measurements. Transition temperature has been reduced by 33 K comparing the unsubstituted sample to that with 5 % substitution.

Introduction

Among the wide variety of coordination compounds there is a class, represented by $3d^4$-$3d^7$ transition metal complexes showing spin transition phenomenon. These compounds can be reversibly switched between two spin states by means of different external stimuli such as temperature, light, pressure and others [1]. Molecular spin crossover (SCO) materials, currently, is an active field of research due to their possible application in nanophotonic, nanoelectronic and nanomechanical devices. Synthesis of nanometer sized spin crossover materials, their manipulation at reduced length scales and the investigation of their size dependent properties contribute to explore their possible practical applications [2,3]. An important challenge in this context is to preserve the bistability and the cooperative spin transition properties during the downsizing of the compound at the nanoscale. The well-known 1,2,4-triazole-iron family of 1D SCO coordination polymers is an appropriate candidate for nanoparticle fabrication. The most fascinating SCO coordination compound from

this family is the $[Fe(H\text{-}trz)_2(trz)](BF_4)$ (H-trz = 1,2,4-4-H-triazole and trz = 1,2,4-triazolato) complex bearing both protonated and deprotonated triazol moiety [4]. This compound is known to preserve its wide thermal hysteresis loop and abrupt spin transition in nanoparticles down to 6 nm [5]. Despite all these advantages the application of such SCO nanoparticles could be accompanied with some difficulties due to the high spin transition temperature which is around 380 K. Consequently, elaboration of spin crossover nanoparticles showing hysteretic behaviour close to room temperature is very important nowadays [6]. It seems that the simplest approach is to modulate the transition temperature in already existing SCO compounds. In the literature, there are several examples describing modulations of spin crossover properties of some 1,2,4-triazole based compounds either by triazole ligand [7-9] or by iron [5,10,13] substitution. This effect was observed not only for bulk materials, but also for nanoparticles [5,11]. As the transition temperature of pure $[Fe(NH_2\text{-}trz)_3](BF_4)_2$ is around 260 K (with hysteresis around 5 K)[12], one can expect a decreasing of the transition temperature when the substitution of 1,2,4-4H-triazole in $[Fe(H\text{-}trz)_2(trz)](BF_4)$ complex by 1,2,4-4-NH_2-triazole takes place.

Here we report the preparation and physical properties of $[Fe(H\text{-}trz)_{2-2x/3}(trz)_{1-x/3}(NH_2\text{-}trz)_x](BF_4)_{1+x/3}$ SCO compounds with x = 0, 0.038, 0.076 and 0.15 for samples **1**-**4**, respectively. The aim is to investigate the influence of the ligand substitution on the size, shape and spin transition properties of these nanoparticles.

Experimental section

Synthesis

All the chemicals and solvents were obtained from Sigma Aldrich and used without any further purification. Spin crossover nanoparticles were prepared using the following procedure: two equivalent microemulsions were prepared mixing together 1.8 ml of Triton X-100, 1.8 ml of 1-hexanol and 7.5 ml cyclohexane. A solution of 211 mg of $Fe(BF_4)_2 \cdot 6H_2O$ in 0.5 ml of H_2O was added dropwise to one microemulsion under stirring and a mixture of 131, 129, 127.7 and 124 mg of 1,2,4-4-H-triazole and 0 (0%), 2 (1,25%), 4 (2.5%) and 8 (5%) mg of 1,2,4-4-NH_2-triazole for sample **1**-**4**, respectively, in 0.5 ml H_2O was added to the other one. These microemulsions were stirred at room temperature until clear solutions were obtained and then quickly mixed together. Several minutes after, the mixture became pink due to the nanoparticle formation. The resulting microemulsion was agitated during 5 hours to ensure that the microemulsion exchange was completed. Then 30 ml of ethanol were added to destroy the microemulsion structure. The obtained nanoparticles were washed several times with ethanol to remove the surfactant and separated by centrifugation at

4000 rpm during 5 minutes. This procedure resulted in nanoparticle yields of 87-90%.

Tentative composition of the samples was obtained thanks to combined C, H, N elemental analysis (Table **1**) and thermogravimetric analysis. Indeed, although elemental analyses confirm the formation of the SCO compounds, exact composition cannot be determined because of possible surfactant and solvent residuals. Thermogravimetric analysis revealed different water amount; 1% for **1** and approximately 4% for **2-4** (**Figure 1**). Thermogravimetric analyses revealed also that samples **2-4** are less stable compared to sample **1** with a decomposition process starting at *ca.* 200ºC. Theoretical quantity of the elements is calculated with respect to the mentioned $[Fe(H\text{-}trz)_{2\text{-}2x/3}(trz)_{1\text{-}x/3}(NH_2\text{-}trz)_x](BF_4)_{1+x/3}$ formulas with the hypothesis that the substitution during micellar exchange occurs proportionally toward protonated and deprotonated triazole ligands.

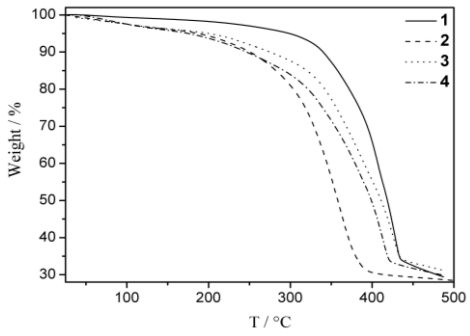

Figure 1. Thermogravimetric analyses for samples **1-4**

Size and physical properties

Transmission electron microscopy (TEM) was carried out using JEOL JEM-1011 (100 kV). TEM samples were prepared by depositing on a carbon coated copper grid (400 mesh) a few drops of the nanoparticles suspended in ethanol. Elemental analysis was carried out using a Flash EA1112 (ThermoFinnigan 2003) apparatus. Magnetic susceptibility of nanoparticle powder samples was measured using a Quantum Design MPMS2 magnetometer in the temperature range from 300 to 400 K under a magnetic field of 1 T with heating-cooling rate of 2 K/min. Optical reflectivity measurements were performed on a stereomicroscope (Motic) equipped with a CCD camera (Moticam 1000) and were monitored in the green optical region. The sample temperature was controlled using a Linkam THMS600 liquid nitrogen cryostat. Temperature change rate was 2 K/min. Dynamic scanning calorimetry was done using NETZSCH Thermal Analysis DSC 204 cell. Thermogravimetric analyses (TGA) data were acquired using a Perkin–Elmer Diamond thermal analyzer. Powder X-ray diffractograms were obtained with a Panalytical MPDPro diffractometer.

Results and discussion

The synthetic method of the nanoparticles was inspired from S. Titos-Padilla and co-workers [13] and consisted to use reverse microemulsion with Triton X-100 as a surfactant and 1-hexanol as a co-surfactant (**Scheme 1**).

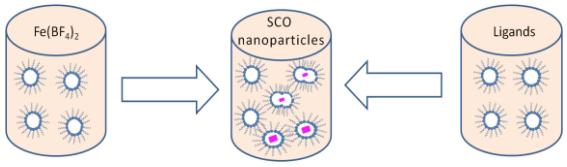

Scheme 1. Schematic representation of the synthetic route

A comparison of the powder X-ray diffraction patterns of **1-4 (Figure 2)** revealed the isostructurality of the samples. However, a broadening of the peaks in **2-4** was observed and rather ascribed to the disordering of the lattice in agreement with the ligand substitution effect even if size and morphology effects are not totally discarded.

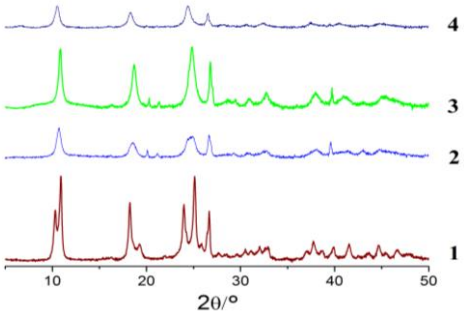

Figure 2. Powder X-ray diffraction patterns of **1-4**.

Particle sizes were determined by transmission electron microscopy (TEM) while their properties were probed by DSC, optical and magnetic measurements. TEM image of the reference $[Fe(Htrz)_2(trz)](BF_4)\cdot 0.2H_2O$ sample **1** shows nanoparticles with platelet-like morphology with average length of ~ 120 ± 9 nm and width of ~ 80 ± 14 nm (**Figure 3**). Temperature dependent magnetic susceptibility measurements carried out on sample **1** are presented in **Figure 4**. For each sample we consider the transition temperature of the second thermal cycle, the first one corresponding to the dehydratation of the sample; all data are gathered in **Table 2**.

The magnetic behavior shows a wide hysteresis of 35 K centered at 365 K ($T_{1/2}\downarrow$ = 348 K and $T_{1/2}\uparrow$ = 383 K) which is very close to the corresponding bulk counterpart [3]. The sample **2** containing 1.25 % of 1,2,4-4-NH_2-triazole shows a transition centred at 360 K with a reduced 20 K hysteresis loop ($T_{1/2}\uparrow$ decreasing to 370 K).

Molecular formula	Mw/ g·mol^{-1}		C%	H%	N%
1 $[Fe(Htrz)_2(trz)](BF_4)\cdot 0.2H_2O$	352.6	Cal.	20.41	2.38	35.73
		Meas.	20.12	2.63	33.92
2 $[Fe(Htrz)_{1.975}(trz)_{0.987}(NH_2\text{-}trz)_{0.038}](BF_4)_{1.013}\cdot 0.9H_2O$	367.6	Cal.	20.18	2.57	35.71
		Meas.	19.93	2.75	33.64
3 $[Fe(Htrz)_{1.95}(trz)_{0.975}(NH_2\text{-}trz)_{0.075}](BF_4)_{1.025}\cdot 0.7H_2O$	364.9	Cal.	20.26	2.65	35.98
		Meas.	19.95	2.48	33.75
4 $[Fe(Htrz)_{1.9}(trz)_{0.95}(NH_2\text{-}trz)_{0.15}](BF_4)_{1.05}\cdot 0.8H_2O$	370	Cal.	19.65	2.87	35.17
		Meas.	19.05	2.68	33.98

Table 1. Elemental analyses and tentative formulas for samples **1-4**

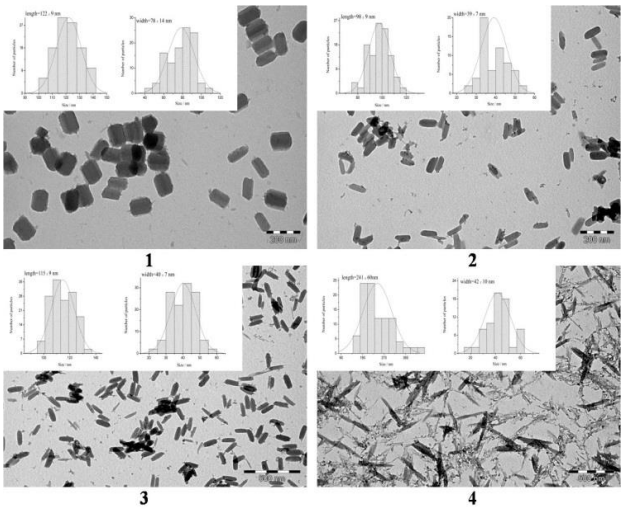

Figure 3. TEM images and size distributions of the synthesized samples **1-4**

It is interesting to notice that the morphology of these nanoparticles is changing also from platelet- to rod-like since the length to width ratio is higher (average length of ~ 100 ± 9 nm and width of ~ 40 ± 7 nm) compared to sample **1.** More significant changes in the spin

crossover behavior were observed in sample **3**. In this case, the transition is more down shifted and centered at 353 K with a narrow 16 K hysteresis loop ($T_{1/2}\downarrow$ = 345 K and $T_{1/2}\uparrow$ = 361 K). As can be seen from the TEM image of this sample, the nanoparticles become longer (average length of ~ 120 ± 9 nm) and the width does not change. This tendency is confirmed for sample **4**, which is composed of needle-like particles with average length of ~ 240 ± 60 nm and width of ~ 40 ± 10 nm. The most drastic SCO property change was observed for the highest ligand substitution with a less abrupt transition centered at 343 K and a hysteresis loop of 13 K ($T_{1/2}\downarrow$ = 337 K and $T_{1/2}\uparrow$ = 350 K). Clearly, the increase of the 1,2,4-4-NH_2-triazole ligand percentage tends to decrease the transition temperature while the hysteresis loop becomes narrow. Similar behaviors have been measured replacing iron atoms by increasing amount of zinc atoms in different size [Fe(H-trz)$_2$(trz)](BF$_4$) nanoparticles.[5,11] Variable temperature optical reflectivity measurements (**Figure 4**) are in good agreement with the magnetic results. The transition temperatures for each sample are indicated in **Table 2**. To make the results more demonstrative, spin transition temperatures depending on 1,2,4-4-NH_2-triazole quantity in the heating and cooling modes are shown in **Figure 5**. The tendency of thermal hysteresis loss can be observed, so that we can expect practically full disappearance of hysteresis when reach room temperature transition. From the other point of view, increasing of the 1,2,4-4-NH_2-triazole quantity may reveal an unexpected behavior of this material.

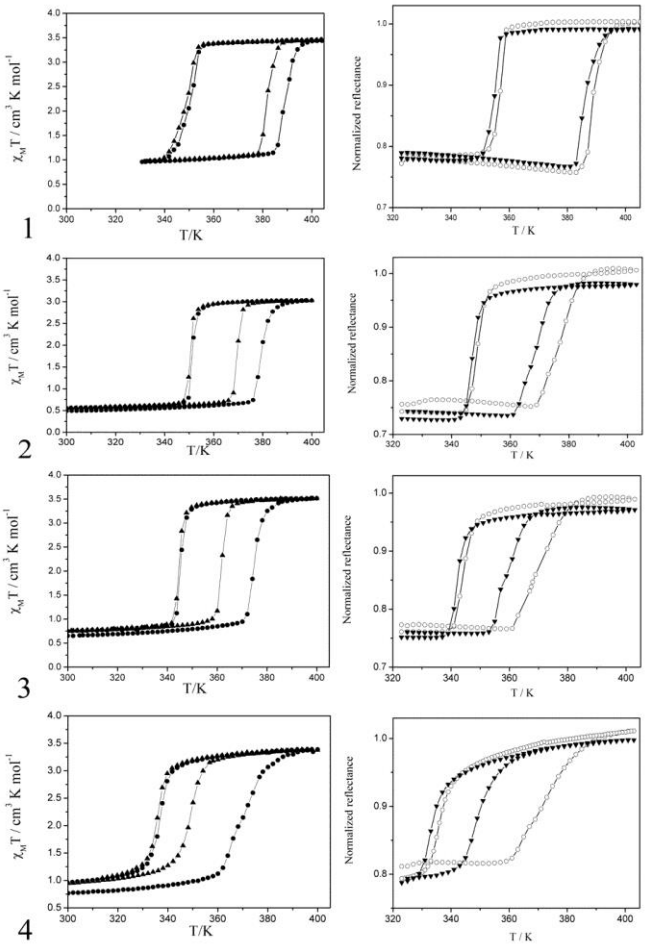

Figure 4. Variable temperature magnetic (left) and optical reflectivity (right) data for samples **1**-**4**. For the magnetic susceptibility graphs, the first cycle is shown in full circles and the second one in triangles. The first cycle in reflectivity curves – empty circles, the second one – triangles.

Sample	Hysteresis [K]		$T_{1/2}\downarrow$ [K]		$T_{1/2}\uparrow$ [K]	
	Magnetism	Reflectivity	Magnetism	Reflectivity	Magnetism	Reflectivity
1	35	32	348	354	383	386
2	20	22	350	347	370	369
3	16	18	345	342	361	360
4	13	16	337	333	350	349

Table 2: Spin crossover properties extracted from magnetic and optical measurements for sample **1**-**4**

Dynamic scanning calorimetry data were collected for sample **4** (**Figure 6**). The

endothermic process is associated with low spin to high spin transition and the exothermic process occurs when the complex returns to the LS state. The enthalpy variation were calculated as 25.1 kJmol^{-1} in heating mode ($T_{1/2}\uparrow$ = 356 K) and 19.7 kJmol^{-1} in cooling mode ($T_{1/2}\downarrow$ = 328 K).

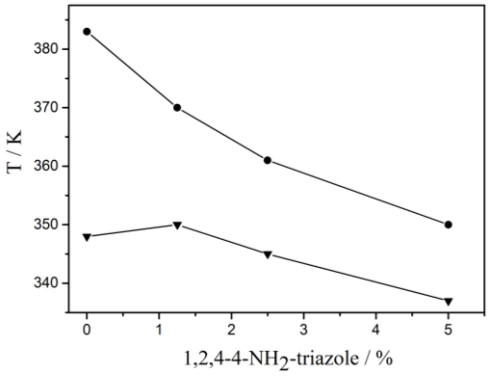

Figure 5. Spin transition temperature versus 1,2,4-4-NH_2-triazole quantity. Heating branch is plotted with full circles and cooling branch with full triangles

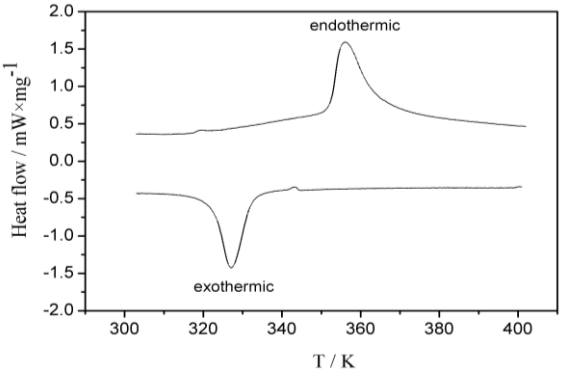

Figure 6. DSC curve of the sample **4**.

These measurements confirm that there is no any other heat transfer besides those belonging to the spin state changes. In other words, we have an individual compound and not a mixture of different complexes.

Conclusions

In summary, we have prepared various iron-triazole SCO nanoparticles using a reverse microemulsion technique and ligand substitution approach. We have shown that the transition temperature can be gradually shifted toward room temperature, with respect to the increasing 1,2,4-4-NH_2-triazole quantity inclusion in the $[Fe(H\text{-}trz)_2(trz)]BF_4$ complex, reducing hysteresis width but still with abrupt spin transition. The modification of the shape of the particles and the concomitant decrease of the transition temperature toward room temperature could be useful for their organization onto surfaces and the elaboration of specific nano-scale devices.

Acknowledgments

This work was financially supported by the project ANR-13-BS07-0020-01. I.S. thanks the French Embassy in Ukraine for financial support. The research has been performed as a part of the GDRI Franco-Ukrainian on molecular chemistry.

References

[1] a) P. Gütlich, A Hauser and H. Spiering, *Angew. Chem., Int.,Ed.*, **1994**, 33, 2024-2054. b) Spin Crossover in Transition Metal Compounds: *Topics in Current Chemistry,* Eds: P. Gütlich and H. A. Goodwin, Springer, Berlin, **2004**.

[2] A. Bousseksou, G. Molnar, L. Salmon et W. Nicolazzi , *Chem. Soc. Rev.* **2011**, 40, 3313-3335.

[3] H. J. Shepherd, G. Molnar, W. Nicolazzi, L. Salmon, A. Bousseksou, *Eur. J. Inorg. Chem*., **2013**, 653–661.

[4] J. Kroeber, J.-P. Audiere, R. Claude, E. Codjovi, O. Kahn, J. G. Haasnoot, F. Groliere, C. Jay and A. Bousseksou, *Chem. Mater.*, **1994**, 6, 1404–1412.

[5] J. R. Galán-Mascarós, E. Coronado, A. Forment-Aliaga, M. Monrabal-Capilla, E. Pinilla-Cienfuegos and M. Ceolin, *Inorg. Chem.*, **2010**, 49, 5706–5714.

[6] a) T. Forestier, S. Mornet, N. Daro, T. Nishihara,S. Mouri, K. Tanaka, O. Fouché, E. Freysz, J.-F. Létard, *Chem. Commun*. **2008**, 4327-4329, b) A. Tokarev, L. Salmon, Y. Guari, G. Molnar, et A. Bousseksou, *New J. Chem*. **2011**, 35, 2081-2088, c) I. Gural'skiy, G. Molnár, I. O. Fritsky, L. Salmon, A. Bousseksou, *Polyhedron*, **2012**, 38, 245-250, d) I. Guralskyi, C. M. Quintero, G. Molnar, I. O. Fritsky, L. Salmon, A. Bousseksou, *Chem. A Eur. J.*, **2012**, 18, 9946-9954.

[7] O. G. Shakirova, L. G. Lavrenova, Y. G. Shvedenkov, V. N. Ikorskii, V. A. Varnek, L. A. Sheludyakova, V. L. Varand, T. A. Krieger and S. V. Larionov, *J. Struct. Chem.*, **2000**, 41, 790–797.

[8] V. A. Varnek, L. G. Lavrenova and S. A. Gromilov, *J. Struct. Chem.*, **1997**, 38, 585–592.

[9] J. Krober, E. Codjovi, O. Kahn, F. Groliere and C. Jay, *J. Am. Chem. Soc.*, **1993**, 115, 9810–9811.

[10] a) O. G. Shakirova, Y. G. Shvedenkov, D. Y. Naumov, L. A. Sheludyakova, L. S. Dovlitova, V. V. Malakhov, L. G. Lavrenova and others, *J. Struct. Chem.*, **2002**, 43, 601–607 b) V. A. Varnek and L. G. Lavrenova, *J. Struct. Chem.*, **1994**, 35, 842–850, c) V. A. Varnek and L. G. Lavrenova, *J. Struct. Chem.*, **1997**, 38, 850–852.

[11] E. Coronado, J. R. Galán-Mascarós, M. Monrabal-Capilla, J. Garciía-Martínez, P. Pardo-Ibánez, *Adv. Mater*. **2007**, 19, 1359-1361.

[12] M. M. Dîrtu, A. Rotaru, D. Gillard, J. Linares, E. Codjovi, B. Tinant and Y. Garcia, *Inorg. Chem.*, **2009**, 48, 7838–7852.

[13] S. Titos-Padilla, J. M. Herrera, X.-W. Chen, J.J. Delgado, E. Colacio, *Angew. Chem. Int. Ed*., **2011**, 50, 3290-3293.